United States Department of Agriculture

NRCS

Natural Resources Conservation Service
National Soil Survey Center
11 Campus Blvd., Suite 200
Newtown Square, PA 19073

Phone: (610) 557-4233
FAX: (610) 557-4136

SUBJECT: MGT – Trip Reports, Lake Sedimentation Surveys, Geophysical Assistance, May 28, 2009.

June 17, 2009

TO: Dr. Patrick Drohan
Assistant Professor of Pedology
Department of Crop and Soil Sciences
The Pennsylvania State University
452 ASI Building
University Park, PA 16802-3504

File Code: 330-20-7

Purpose:
The purpose of this GPR study was to determine depths to lake-bottom sediments within Black Moshannon Lake, which is located in Black Moshannon State Park near Phillipsburg, Pennsylvania.

Participants:
Jim Doolittle, Research Soil Scientist, USDA-NRCS, Newtown Square, PA
Emilie Erich, Graduate Student, Department of Crop and Soil Science, Pennsylvania State University, University Park, PA
Mary Kay Lupton, Project Assistant, Department of Crop and Soil Science, Pennsylvania State University, University Park, PA

Activities:
The survey was completed on May 28, 2009.

Results:
1. The radar survey of Black Moshannon Lake was completed in one day. Twenty-one, sinuous traverses were made across Black Moshannon Lake with GPR. Water depths were recorded at an astonishing, 244,126 points. The coordinates of each of these points were recorded with GPS. Based on a preliminary interpretation of radar data, the average depth of Black Moshannon Lake is 1.87 m with a range of about 0.58 to 4.10 m.

2. GPR is an excellent tool for bathymetric surveys of freshwater lakes and reservoirs. The lake bottom was clearly identifiable on all radar records. The depth of the water was estimated with reasonable certainty at most observation points.

3. The lake-bottom sediments were penetrable with GPR. However, within the lake-bottom sediments, the actual depth of penetration as well as the velocity of propagation varied with the clay, organic matter, and moisture contents.

4. All interpreted radar data have been compiled into a spreadsheet and forwarded to you for analysis. Copies of the Google Earth images, showing the lake, locations of traverse lines, and interpreted depths to the lake-bottom sediments along these lines, have also been forwarded to you.

It was my pleasure to participate in this study and to conduct fieldwork with your graduate student and research assistant.

With kind regards,

Jim Doolittle
Research Soil Scientist
National Soil Survey Center

cc:
S. Carpenter, MLRA Office Leader, NRCS, 75 High Street, Room 301, Morgantown, WV 26505
K. Hipple, Acting Director, National Soil Survey Center (NSSC), NRCS, Federal Building, Room 152, 100 Centennial Mall North, Lincoln, NE 68508-3866
M. Golden, Director, Soils Survey Division, NRCS, Room 4250 South Building, 14th & Independence Ave. SW, Washington, DC 20250
W. Tuttle, Soil Scientist (Geophysical), NSSC, NRCS, P.O. Box 60, 207 West Main Street, Rm. G-08, Federal Building, Wilkesboro, NC 28697
L. West, National Leader, Soil Survey Research and Laboratory Staff, NSSC, NRCS, Federal Building, Room 152, 100 Centennial Mall North, Lincoln, NE 68508-3866
E. White, State Soil Scientist, NRCS, One Credit Union Place, Suite 340, Harrisburg, PA 17110-2993

Background:
Black Moshannon Lake is located in Centre County, approximately eight miles east of Phillipsburg, Pennsylvania. At an elevation of about 1,900 feet (580 m) the 250-acre (101-ha) lake is located in a natural basin in the Allegheny Plateau, just west of the Allegheny Front. The lake was formed by a dam on Black Moshannon Creek, and is fed by several springs and small streams. Peatlands extend along large segments of the shoreline. Sedimentation is a major cause of the reduction in lake's storage capacity. The primary objective of this bathymetric survey is to determine water depths. This data can be used to estimate current reservoir capacity, changes that have occurred in storage volume, and the volume of accumulated sediments.

To determine sedimentation rates and changes in lake-bottom topography, depth soundings are typically taken at select locations within lakes (Truman et al., 1991). This process is slow, tedious, and costly. Improved methods are needed to expedite the completion of these surveys and to provide more comprehensive coverage of lakes and reservoirs. Acoustical sounding systems (fathometer) are often used for freshwater bathymetric surveys. However, fathometers have difficulties resolving gradational lake-bottom contacts and penetrating aquatic vegetation or layers of organic materials (Kovacs, 1991; Sellmann et al., 1992). Sellmann et al. (1992) recognized that because of the greater electrical than acoustical contrasts in most lake-bottom sediments, greater resolution and sub-bottom information can be achieved with GPR than acoustical methods. Delaney et al. (1992) concluded, however, that the combined use of acoustical and GPR methods can provide improved and complementary sub-bottom information.

Ground-penetrating radar measures the time it takes for a shortwave electromagnetic pulse to travel from a radar antenna to a subsurface interface and back to the antenna after being reflected off the interface. The greater the contrast in the electrical properties of the materials at the interface, the stronger the reflected pulses will be. High conductivity materials lead to greater attenuation of radar energy than low conductivity materials, therefore, higher conductivity materials lead to shallower effective exploration depths with GPR. Typical effective exploration depths are a few meters, but can be greater than 30 meters if the geologic setting is favorable (i.e., sediments with primarily low conductivity such as dry sands) (Barr, 1993).

GPR has been used in freshwater bathymetric surveys. Truman et al. (1991) used GPR to map the depth of a reservoir in west-central Georgia, relying on differences in the relative dielectric permittivity of water versus lake-bottom sediments to provide strong and easily recognized reflections. When compared to control measurements, water depths interpreted from radar records showed a strong linear relationship with an R^2 value of 0.989. Barr (1993) used GPR to investigate the hydrogeology of freshwater lakes in Florida, including disturbance of lake-bottom sediments. Other examples of the use of GPR to map freshwater bottom-topography and -sediments include studies conducted by Buynevich and Fitzgerald (2003), Moorman (2001), Moorman and Michel (1997), Mellett (1995), Sellmann et al. (1992), Izbicki and Parker (1991), Kovacs (1991), and Haeni et al. (1987). Ground-penetrating radar has also been used to measure stream-channel cross sections (Annan and Davis, 1977; Spicer et al., 1997; Stevens et al., 2009) and scours at bridge piers in riverbed (Gorin and Haeni, 1989). In the aforementioned studies, GPR identified the water-sediment boundary to depths as great as 10 m and provided highly resolved, bathymetric cross-sections.

Powers and Haeni (1999) compared the use of continuous seismic-reflection profiling and GPR to delineate the types and thickness of sedimentary units in a small pond in eastern Massachusetts. These geophysical tools provided complementary information and detected similar interfaces. Haeni et al. (1987) and Powers and Haeni (1999) estimated the thickness of organic deposits within portions of lake basins. In these studies, the water/organic matter and the organic matter/mineral soil interfaces were electrically contrasting and provided excellent radar reflections. However, in some portions of the profiled lakes, the organic matter/mineral soil interface was not interpretable because of admixtures of silts and clays.

Equipment:
The radar unit is the TerraSIRch Subsurface Interface Radar (SIR) System-3000 (SIR-3000), manufactured by Geophysical Survey Systems, Inc. (GSSI; Salem, NH).[1] The SIR-3000 consists of a digital control unit (DC-3000)

[1] Manufacturer's names are provided for specific information; use does not constitute endorsement.

with keypad, SVGA video screen, and connector panel. A 10.8-volt lithium-ion rechargeable battery powers the system. The SIR-3000 weighs about 4.1 kg (9 lbs). The center frequency of the antenna used in this investigation is 70 MHz. Daniels (2004) and Jol (2008) discuss the uses and operation of GPR.

All radar records were processed with the RADAN for Windows (version 6.6) software developed by GSSI. [1] Processing included: header editing, GPS positioning, time zero adjustments, and range gain adjustments.

Recent technical developments allow the integration of GPR and GPS data (Doolittle et al., 2009). This integration effectively geo-references each scan on a radar record. The scanning rate was set to 30 scan/sec. This scanning rate resulted in 244,126 geo-referenced measurement points. The GPS coordinates were recorded with a Trimble AgGPS114 L-band DGPS (differential GPS) antenna (Trimble, Sunnyvale, CA).[1]

Using the *Interactive 3D Module* of the RADAN for Windows (version 6.6) software program, depths to subsurface interfaces can be interpreted, automatically picked and outputted to a layer file (X, Y, Z format; containing latitude, longitude, and depth). The synergism of these technologies permits the collection of large, tabular, georeferenced GPR data sets, which can be stored, manipulated, analyzed, and displayed in GIS.

Survey Procedures:
The radar system was mounted in a boat, which was powered by an electrical motor. The 70 MHz antenna was extended (using wooden doles) over the water on one side of the boat. The antenna was positioned about 6 inches above the water. The proximity of the antenna to the boat did not create any noticeable ringing or interference to the radar signal. The boat, moving at a slow speed of advance, made multiple traverses across Black Moshannon Lake. Because of very shallow water depths and the presence of aquatic vegetation, the upper reaches and other shallow areas of the lake could not be surveyed with GPR by boat.

Ground Penetrating Radar:
Ground-penetrating radar is an impulse radar system that is specially designed to penetrate earthen materials. Electromagnetic wave propagation is affected by contrast in electromagnetic properties (dielectric permittivity, electrical conductivity, and magnetic susceptibility) of the profiled material(s) (Daniels, 2004). Electromagnetic energy is directed into the subsurface by a transmitting antenna. When propagated waves of electromagnetic energy encounter an interface separating layers of contrasting electromagnetic properties a portion of the transmitted wave is reflected back to the antenna. The reflected energy is detected by the receiving antenna and recorded.

Ground-penetrating radar is a time scaled system. This system measures the time that it takes electromagnetic energy to travel from the antenna to an interface (e.g., lake bottom, stratigraphic layer) and back. To convert the travel time into a depth scale, either the velocity of pulse propagation or the depth to a reflector must be known. The relationships among depth (D), two-way pulse travel time (T), and velocity of propagation (v) are described in the following equation (after Daniels, 2004):

$$D = v\,(T/2) \qquad [1]$$

The velocity of propagation is principally affected by the dielectric permittivity (E) of the profiled material(s) according to the equation (after Daniels, 2004):

$$v = C/\,(E)^{1/2} \qquad [2]$$

Where C is the velocity of propagation in a vacuum (0.3 m/nanosecond). Typically, v is expressed in meters per nanosecond (m/ns). A nanosecond is one billionth of a second. The amount and physical state of water (temperature dependent) have the greatest effect on the dielectric permittivity of a material.

Interpretations of the radar records were accomplished by using a propagation velocity of 0.033 m/ns and a dielectric permittivity of 80 for water (Morey, 1974). Slight variations in velocity of propagation are known to

occur in lake waters because of differences in the suspended sediment concentration (Spicer and Costa, 1997). A set range of 340 ns provided a maximum profiling depth of 4.54 m.

At two calibration points on Black Moshannon Lake, depths to the lake-bottom sediments were measured and compared with the depths interpreted from the radar imagery and equation [1]. Depths to the lake-bottom sediments were measured with a stadia rod. At these points, the depths to the lake-bottom sediments were 82 to 238 cm. At the two calibration points, differences between measured and interpreted depths were 2 and 4 cm.

Differences between measured and interpreted depths to the lake-bottom sediments are attributed to slight spatial discrepancies between the point of stadia and radar measurements, the area scanned and the resolution of the GPR. Energy is transmitted from the radar antenna in a conical beam. The radar measures a circular footprint area beneath the antenna. This footprint area can be estimated by the formula (Kovacs, 1991):

$$2 \sin^{-1} (1/E) \qquad [3]$$

Kovacs (1991) noted that for an antenna resting on water, as a rule of thumb, the beam width is approximately equal to 0.2D, where D is the water depth. Using this approximation, at the 2 calibration sites, the beam width scanned by GPR varied from about 16 cm (water depth of 82 cm) to 48 cm (water depth of 238 cm).

On radar records, reflections from interfaces spaced (vertically) closer than ½ wavelength apart are indistinguishable due to constructive and destructive interference (Daniels, 2004). Daniels (2004) used the following equation to show the relationship between velocity of propagation (v), antenna center frequency (f), and wavelength (λ):

$$\lambda = v/f \qquad [4]$$

Equation [4] shows that the propagated wavelength will decrease with decreasing propagation velocity and increasing antenna frequency. Using equation [4] and an average velocity of 0.033 m/ns results in wavelengths of about 47 cm (18 inches) with a frequency of 70 MHz (assuming that the center frequency of the antenna is not reduced because of impedance loading with the fresh water). As a consequence, layers spaced closer than about 24 cm apart are difficult to identify on radar records collected with the 70 MHz antenna.

Interpretations:

Using the *Interactive 3D Module* of RADAN, depths to the lake-bottom sediments reflector were quickly and effortlessly picked and recorded in layer files. Based on 244,126 interpreted measurements made along the 21 traverse lines, the average depth to this contact is about 187 cm with a range of about 58 to 410 cm. Figure 1 is a Google Earth image of the area that was traversed with GPR at Black Moshannon Lake. The locations and the interpreted depths to lake-bottom sediments along the traverse lines are shown on this image. As evident on this image, water depths increase towards the north end of the lake (right) and lake-bottom sediments become increasingly shallower towards the south (left) and especially in the two branching, southern arms of the lake.

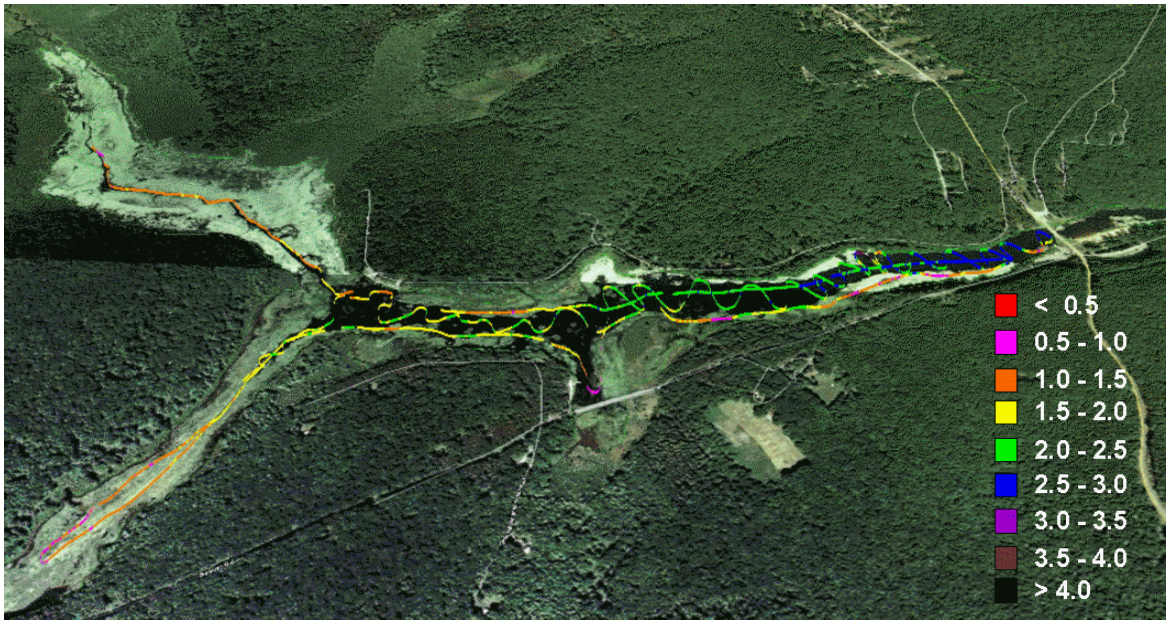

Figure 1. In this Google Earth image of Black Moshannon Lake, the locations of the georeferenced GPR traverse lines are shown. Colors indicate the depths (in meters) to lake-bottom sediments.

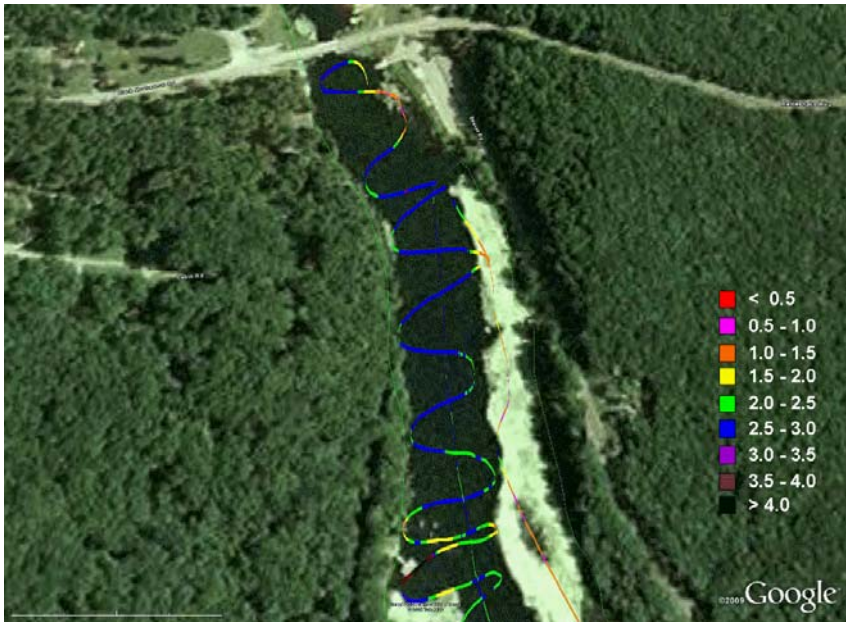

Figure 2. In this Google Earth image of the northern-most surveyed portion of Black Moshannon Lake, the locations of the georeferenced GPR traverse lines are shown. Colors indicate the depths (in meters) to lake-bottom sediments. This is the deepest portion of the lake that was surveyed with GPR.

Figures 2, 3, and 4 provide different perspectives and a closer look at the recorded depths to lake-bottom sediments in the northern, central, and southern portions of Black Moshannon Lake, respectively. The general depth to lake-bottom sediments decreases from north to south. The expansion of sphagnum moss into the lake is evident in these images as one proceeds from north to south. In 1994, 1,592 acres (644 ha) were set aside and protected as the "Black Moshannon Bog Natural Area. Since then, the total area of “bog” that is protected as a *Natural Area* within the park has increased to 1,992 acres (806 ha).

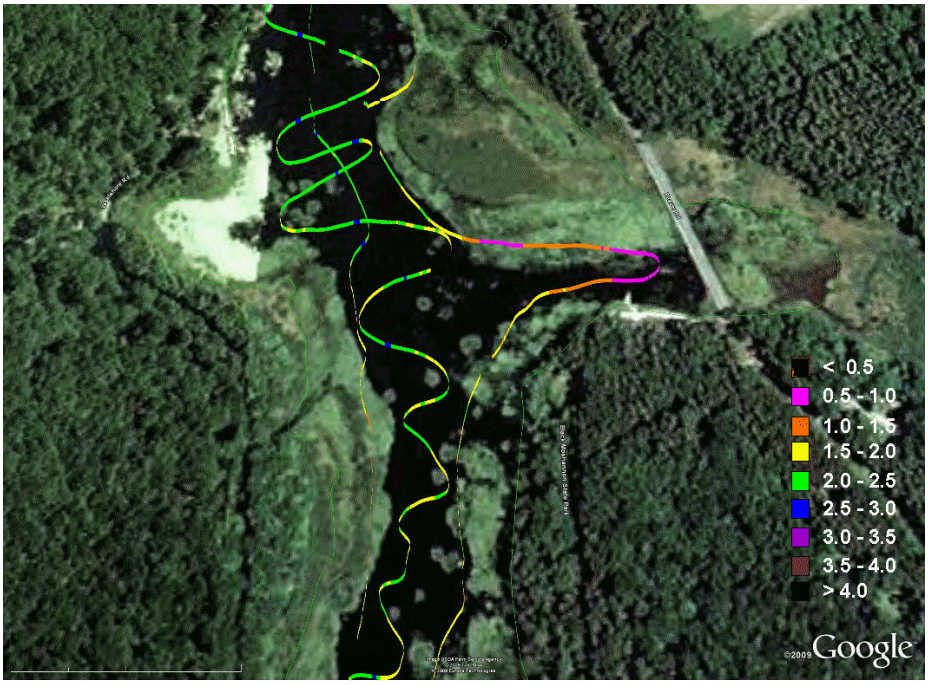

Figure 3. In this Google Earth image of the mid-portion of Black Moshannon Lake, the locations of the georeferenced GPR traverse lines are shown. Colors indicate the depths (in meters) to lake-bottom sediments. In general (excluding embayment areas), this section has intermediate depths to lake-bottom sediments.

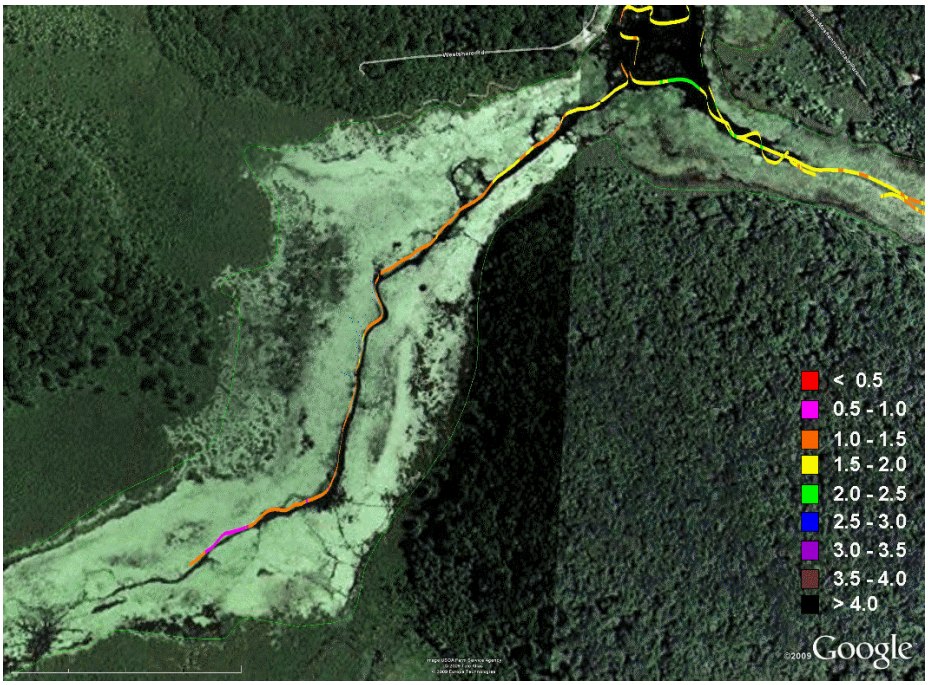

Figure 4. In this Google Earth image of the southern-most surveyed portion of Black Moshannon Lake, the locations of the georeferenced GPR traverse lines are shown. Colors indicate the depths (in meters) to lake-bottom sediments. This is the shallowest portion of the lake that was surveyed with GPR. Note how this portion is largely occupied by aquatic plants and organic sediments.

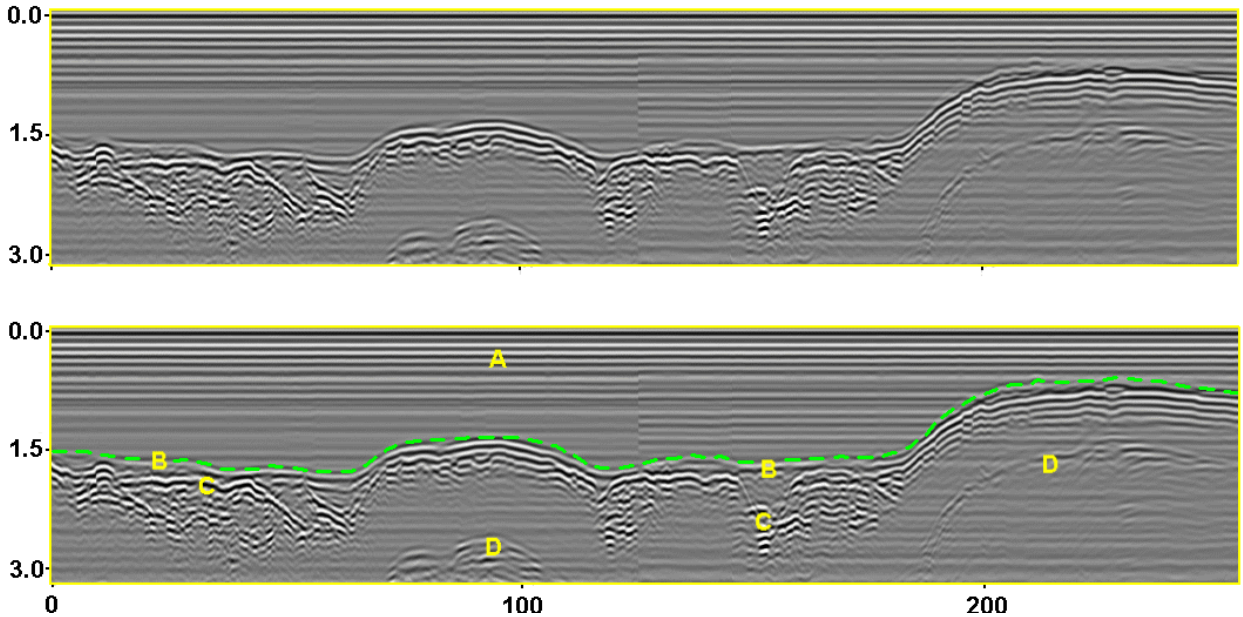

Figure 5. Two renditions of the same radar record from Black Moshannon Lake are shown: an un-annotated (upper) and an annotated (lower) record. All scales are expressed in meters.

Radar records collected on Black Moshannon Lake were of good quality and interpretable. Figure 5 contains to renderings of the same radar record that was collected with the 70 MHz antenna over Black Moshannon Lake. The radar record appearing in Figure 5 has been compressed and reduced in size to accommodate the page. The vertical and horizontal scales are expressed in meters. In Figure 5, the lower rendition has been annotated. The lake bottom is apparent across both renditions of this radar record and varies in depth from about 60 to 170 cm. In the lower, annotated rendition, a green-colored, segmented line approximates this interface.

In both renditions of the radar record shown in Figure 5, the horizontal bands at the top of the radar record (see "A" in lower rendition) represents reflections from the lake's surface and multiples. The multiple, continuous horizontal bands across the top of the radar record are the result of antenna "ringing". Ringing is caused, in part, by an impedance mismatch between the antenna and the water (Sellmann et al., 1992). Noise, associated with the antenna's proximity to the boat, is another source of these multiple bands. The first series of continuous, moderate to high amplitude, subsurface bands (see "B" in lower rendition) represents the lake bottom. On this radar record, this interface varies in depth from about 60 to 170 cm). A lower group of reflectors (see "C") represents the base of the post-impoundment sediments and the contact with the original lake bottom materials. Reflections from the original bottom sediments have higher signal amplitudes than reflections from the overlying, present lake-bottom. Higher signal amplitudes suggest interfaces that separate more contrasting materials. It is inferred from these dissimilar signal amplitudes that the recently deposited lake bottom materials are less dense, have higher moisture contents, and are most likely composed of organic and/or organic-mineral soil materials (organics will have higher moisture contents and therefore provide a less contrasting interface with the overlying water column). The underlying original bottom materials have noticeably higher signal amplitudes and a more irregular topography than the overlying reflectors from the more recently deposited sediments. A "double-return echo" from the lake bottom has been identified (see "D") in the lower rendition. This group of multiple reflectors is a form of noise and should be ignored. Lake bottom multiples (see *D* in Figure 5) were observed on some radar records. They represent secondary reflections from the lake bottom. Multiples have the same shape as the lake bottom but occur at twice the travel time to the bottom reflection (Moorman, 2001).

With the 70 MHz antenna the lake-bottom sediments were penetrated. However, as no borings were made through these sediments at the time of the survey, the identities of these layers were not verified and the thickness of lake bottom sediments can not be measured. If the textural composition of these layers can be estimated, approximations of the relative thickness of the post-impoundment sediments can be made.

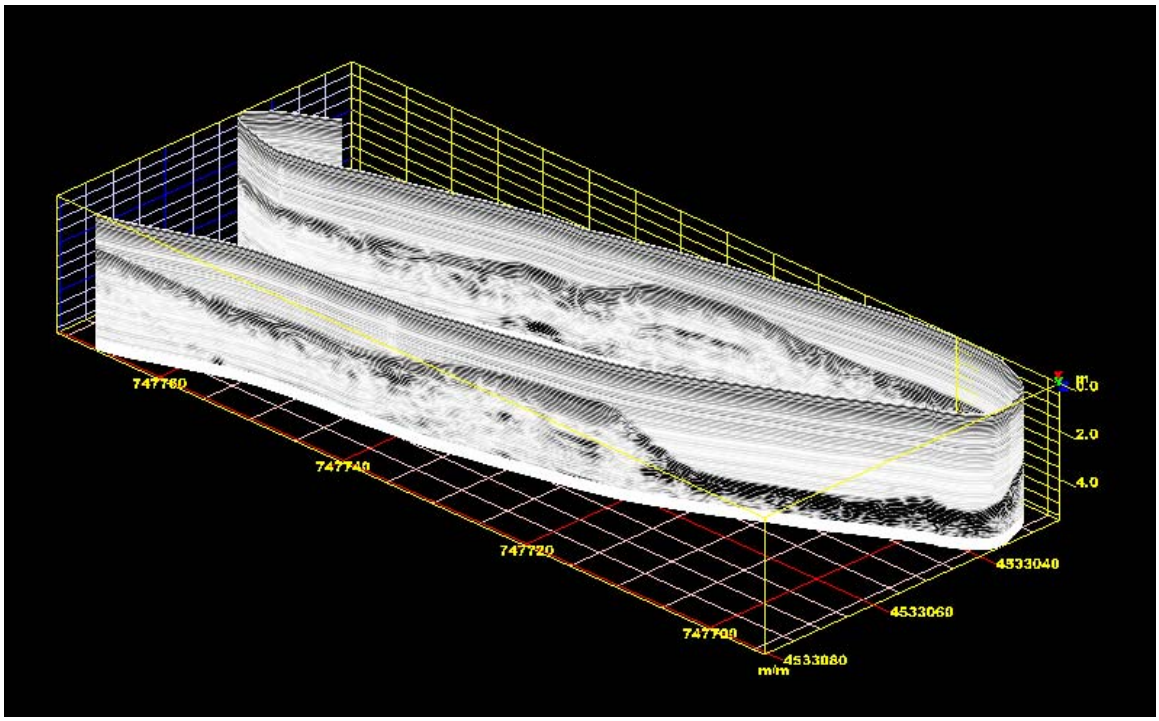

Figure 6. This 3D pseudo image of a radar record, which was collected in the northern portion of Black Moshannon Lake, shows a deeper area with high-amplitude reflections (colored black), which is indicative of an interface separating more contrasting materials. All scales (depth and UTM) are expressed in meters.

Figures 6 and 7 are three-dimensional (3D) pseudo-images of radar records that were collected in the northern and southern portions of the lake, respectively. In both images, the contact between the water and the lake bottom provides a continuous, easily recognizable interface. Contrast in the amplitude of this reflector suggests variations in bottom materials. In Figure 6, along this interface, an area of higher amplitude reflections is evident and suggests a portion composed of more contrasting materials, perhaps bedrock. The thickness of post-impoundment sediments is relatively thin in this portion of the lake as the interface between the original and present bottom is closely-spaced or lacking.

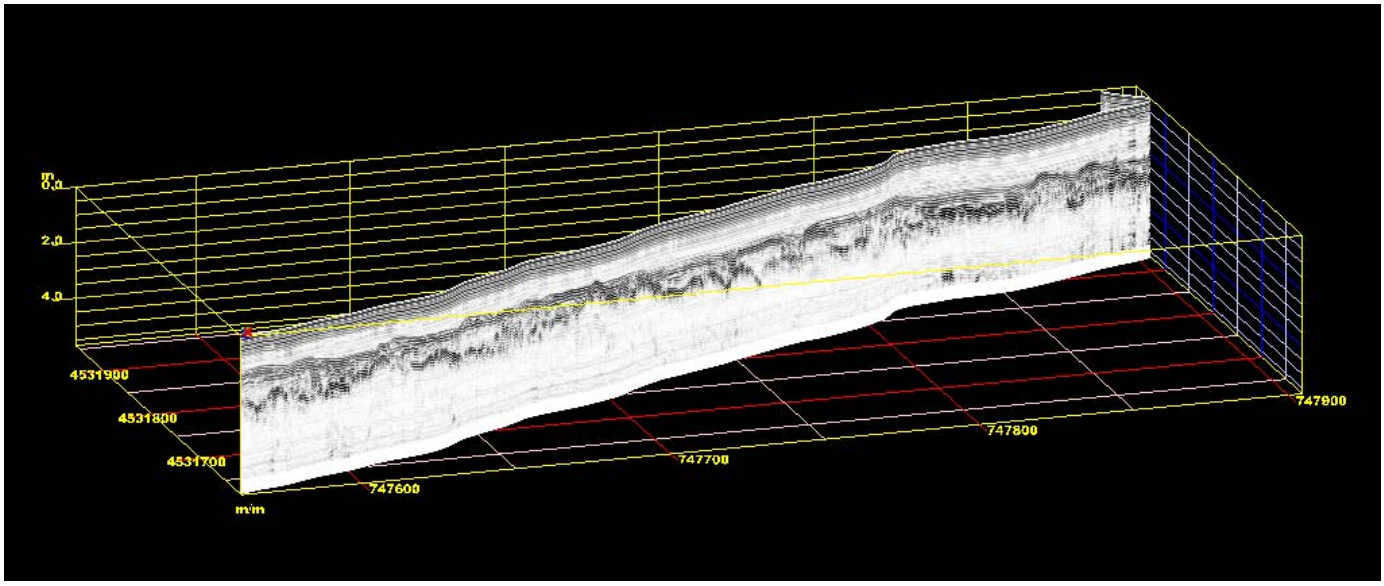

Figure 7. In this 3D pseudo image of a radar record from the shallower southern portion of Black Moshannon Lake, to separate interfaces are evident: the smooth water - bottom sediment interface and the more irregular bottom sediment - original bottom interface. All scales (depth and UTM) are expressed in meters.

In Figure 7, the depth to bottom sediments is noticeably shallower than in the pseudo-image shown in Figure 6. The interface separating the water from the lake-bottom sediments is relatively smooth and even. In Figure 7, reflections from the original bottom sediments are more widely spaced from the overlying lake-bottom surface, suggesting a greater infilling or deposition of materials. Judging from this separation, the thickness of post-impoundment sediments is relatively thick in this portion of the lake. The original bottom provides higher amplitude reflections and has a more irregular topography than the present surface of the lake-bottom sediments. Based on reflection characteristics the extent and relative thickness of different sub-bottom sediments can be inferred. In general, horizontal laminar reflectors are associated with recent sediments. Low amplitude lake/bottom reflections suggest a transitional layer of soft, fluid sediments composed of water saturated organic or organic/mineral materials. As no borings were made at the time of the GPR survey, the identity of these layers remains in doubt.

References

Annan, A. P. and J. L. Davis, 1977. Impulse radar applied to ice thickness measurements and freshwater bathymetry. 63-65 pp. *IN*: Report of Activities, Part B. Geol. Survey of Canada. Paper 77-1B. Ottawa, Canada.

Barr, G.L., 1993. Application of Ground-Penetrating Radar Methods in Determining Hydrogeologic Conditions in a Karst Area, West-Central Florida. *US Geological Survey Water-Resources Investigations Report 92-4141*.

Buynevich, I.V., and D.M. Fitzgerald, 2003. High-Resolution Subsurface (GPR) Imaging and Sedimentology of Coastal Ponds, Maine, USA: Implications for Holocene Back-Barrier Evolution. *Journal of Sedimentary Research* 73(4): 559-571.

Daniels, D. J., 2004. *Ground Penetrating Radar; 2nd Edition*. The Institute of Electrical Engineers, London, United Kingdom.

Delaney, A. J., P. V. Sellmann, and S. A. Arcone. 1992. Sub-bottom profiling: a comparison of short-pulse radar and acoustic data. 149-157 pp. *IN*: P. Hanninen and S. Autio (ed.) Fourth International Conference on Ground-Penetrating Radar. 7 to 12 June 1992. Rovaniemi, Finland. Geological Survey of Finland, Special Paper 16.

Doolittle, J., D. Surabian, S. McVey, and D. Parizek, 2009. Three “G’s” for Soil-Bedrock Depth Interpretations. *Soil Survey Horizons* 50(1): 25-29.

Gorin, S. R., and F. P. Haeni, 1989. Use of surface-geophysical methods to assess riverbed scour at bridge piers. *US Geological Survey Water-Resources Investigation Report 88-4212*. Hartford, Connecticut. 33 p.

Haeni, F. P., McKeegan, D. K., and D. R. Capron, 1987. Ground-penetrating radar study of the thickness and extent of sediments beneath Silver Lake, Berlin and Meriden, Connecticut. *US Geological Survey Water-Resources Investigation Report 85-4108*. Hartford, Connecticut. 19 p.

Izbicki, J. A. and G. W. Parker, 1991. Water depth and thickness of sediment in Reservoirs 1 and 2, Framingham and Ashland, Massachusetts. US Geological Survey Open-File Report 91-508. 18 p.

Jol, H., 2008. *Ground Penetrating Radar: Theory and Applications*. Elsevier Science, Amsterdam, The Netherlands.

Kovacs, A., 1991. Impulse radar bathymetric profiling in weed-infested fresh water. *CRREL Report 91-10*. U. S. Army Corps of Engineers, Cold Regions Research and Engineering Laboratory, Hanover New Hampshire.

Mellett, J. S., 1995. Profiling of ponds and bogs using ground-penetrating radar. Journal of Palelimnology. 14:233-240.

Moorman, B. J., 2001. Ground-penetrating radar applications in paleolimnology. 1-25 pp. *IN*: Last, W.M. and J. P. Smol (eds.). Tracking Environmental Change using Lake Sediments: Physical and Chemical Techniques. Kluwer Academic Publishers, Dordrecht, The Netherlands.

Moorman, B. J. and F. A. Michel, 1997. Bathymetric mapping and sub-bottom profiling through lake ice with ground-penetrating radar. *Journal of Palelimnology* 18:61-73.

Morey, R. M., 1974. Continuous subsurface profiling by impulse radar. 212-232 pp. *IN*: Proceedings, ASCE Engineering Foundation Conference on Subsurface Exploration for Underground Excavations and Heavy Construction, held at Henniker, New Hampshire. Aug. 11-16, 1974.

Powers, C. J., and F. P. Haeni, 1999. Integrated use of continuous seismic-reflection profiling and ground-penetrating radar methods at John’s Pond, Cape Cod, Massachusetts. 359-688 pp. *IN*: Powers, M. H., L. Cramer, and R. S. Bell (eds.). Proceedings of the Symposium on the Application of Geophysics to Engineering and Environmental Problems. Annual meeting of the Environmental and Engineering Geophysical Society. March 14-18, 1999, Oakland, CA.

Sellmann, P. V., A. J. Delaney, and S. A. Arcone, 1992. Sub-bottom surveying in lakes with ground-penetrating radar. *CRREL Report 92-8*. U. S. Army Corps of Engineers, Cold Regions Research and Engineering Laboratory, Hanover, New Hampshire.

Spicer, K. R., J. E. Costa, and G. Placzek. 1997. Measuring flood discharge in unstable stream channels using ground-penetrating radar. *Geology* 25(5): 423-426.

Stevens, C. W., B. J. Moorman, S. M. Solomon, and C. H. Hugenholtz, 2009. Mapping subsurface conditions within the near-shore zone of an Arctic delta using ground penetrating radar. *Cold Regions Science and Technology* 56: 30–38.

Truman, C. C., L. E. Asmussen, and H. D. Allison, 1991. Ground-penetrating radar: A tool for mapping reservoirs and lakes. *Journal of Soil and Water Conservation* 46(5):370-373.